J Neuropathol Exp Neurol
Vol. 76, No. 7, July 2017, pp. 595–604
doi: 10.1093/jnen/nlx040

ORIGINAL ARTICLE

Characterization of 2 Novel Ependymoma Cell Lines With Chromosome 1q Gain Derived From Posterior Fossa Tumors of Childhood

Vladimir Amani, BS, Andrew M. Donson, BS, Seth C. Lummus, MD, Eric W. Prince, BS, Andrea M. Griesinger, MS, Davis A. Witt, MS, Todd C. Hankinson, MD, Michael H. Handler, MD, Kathleen Dorris, MD, Rajeev Vibhakar, MD, Nicholas K. Foreman, MD, and Lindsey M. Hoffman, DO

Abstract

Ependymoma (EPN) is a common brain tumor of childhood that, despite standard surgery and radiation therapy, has a relapse rate of 50%. Clinical trials have been unsuccessful in improving outcome by addition of chemotherapy, and identification of novel therapeutics has been hampered by a lack of in vitro and in vivo models. We describe 2 unique EPN cell lines (811 and 928) derived from recurrent intracranial metastases. Both cell lines harbor the high-risk chromosome 1q gain (1q+) and a derivative chromosome 6, and both are classified as molecular group A according to transcriptomic analysis. Transcriptional enrichment of extracellular matrix-related genes was a common signature of corresponding primary tumors and cell lines in both monolayer and 3D formats. EPN cell lines, when cultured in 3D format, clustered closer to the primary tumors with better fidelity of EPN-specific transcripts than when grown as a monolayer. Additionally, 3D culture revealed ependymal rosette formation and cilia-related ontologies, similar to in situ tumors. Our data confirm the validity of the 811 and 928 cell lines as representative models of intracranial, posterior fossa 1q+ EPN, which holds potential to advance translational science for patients affected by this tumor.

Key Words: Cell line, Ependymoma, Chromosome 1q gain.

From the Morgan Adams Foundation Pediatric Brain Tumor Research Program (VA, AMD, EWP, AMG, DAW, KD, RV, NKF, LMH); Department of Pathology (SCL); and Department of Neurosurgery, University of Colorado Anschutz Medical Campus (TCH, MHH, NKF); and Children's Hospital Colorado (VA, AMD, SCL, EWP, AMG, DAW, TCH, MHH, KD, RV, NKF, LMH), Aurora, Colorado.

Send correspondence to: Lindsey M. Hoffman, DO, Children's Hospital Colorado, 13123 E. 16th Ave, Aurora, CO 80045; E-mail: lindsey.hoffman@childrenscolorado.org

Vladimir Amani and Andrew Donson contributed equally to this work.

The authors declare that they have no competing interests.

Funding was kindly provided by Hyundai Hope on Wheels, Morgan Adams Foundation and the Tanner Seebaum Foundation. The Genomics and Microarray Shared Resource and the Histology Shared Resource receive direct funding support from the National Cancer Institute through the University of Colorado Cancer Center Support Grant (P30CA046934).

Supplementary Data can be found at http://www.jnen.oxfordjournals.org.

INTRODUCTION

Ependymoma (EPN) is the third most common pediatric CNS tumor. Nearly half of newly diagnosed patients will recur after maximally safe surgical resection and focal radiation, and most patients who relapse will not be cured (1, 2). Ninety percent of childhood EPNs arise intracranially, and approximately two thirds of these occur in the posterior fossa (PF) (3). Novel therapeutic strategies are needed for EPN, but development of such agents has been hampered by a lack of cell lines, xenografts, or other animal models. Clinical trials based on preclinical modeling have been proposed for other pediatric brain tumors. Preclinical high-throughput drug screens using EPN cell lines have the potential to inform the design of such trials for EPN.

The prognostic impact of tumor grade (World Health Organization [WHO] grade II versus III) on EPN outcome is not clear (4). Recent studies have focused on molecularly classifying EPNs and have defined distinct molecular groups. The 2 main groups of PF EPNs are groups A and B, which have distinct biological phenotypes and clinical outcomes. Group A tumors exhibit more aggressive biology and a higher risk of recurrence (5–7). Numerous molecular markers have been reported to affect prognosis; to date, gain of chromosome 1q (1q+) has proven to be the most consistent poor prognostic marker. 1q+ is commonly found in WHO grade III tumors (2, 8, 9) and was confirmed by multiple groups as an independent adverse prognostic marker not only for recurrence risk, but also overall survival (10, 11). PF EPNs are distinct from supratentorial (ST) EPNs and harbor no driving mutations, unlike ST EPNs that often harbor *RELA* or *YAP* fusions (4). Children with 1q+ EPNs do not seem to benefit from the standard therapeutic approach that includes surgery and radiation.

Here, we describe 2 new pediatric EPN cell lines (811 and 928) that may serve as powerful research tools. We show that these cells lines, harvested from children with recurrent intracranial metastatic EPNs, show morphological, genetic, and molecular similarities to their primary disease. Their chromosomal gain of 1q and retained characteristics of PF molecular group A make them ideal tools to identify clinically relevant vulnerabilities in high-risk EPN.

MATERIALS AND METHODS

Cell Line Establishment and Propagation

Cell line 811 was derived from a 6-year-old boy, who received standard focal radiation therapy at diagnosis. He experienced local recurrences at 9 and 16 months and intracranial metastatic recurrences at 31 and 36 months from diagnosis; cell lines were established from the third and fourth recurrences (811_4 and 811_5). Cell line 928 was derived from a 3-year-old boy, who received therapy on a clinical trial (ACNS0831) with chemotherapy and radiation therapy at diagnosis. He experienced local recurrence at 32 months and metastatic recurrences to the spine at 34 and 41 months from diagnosis; cell lines were derived from spinal recurrences (928_3 and 928_4). Fresh tumor samples were collected during surgery in Neurobasal-A media (Life Technologies, Grand Island, NY) and immediately disaggregated as described previously (12). Briefly, a razor was used to mince resected tumor that was further triturated by vigorous pipetting. A 70-μm cell strainer was used to filter out clumped tumor, resulting in a single-cell suspension. Cells were plated in Optimem media supplemented with 15% fetal bovine serum (Gibco, Carlsbad, CA) and cultured in either (1) ultra-low attachment plates (Corning, Inc., Corning, NY) to form nonadherent cultures referred to as "3D cultures" in the text, or (2) using standard tissue culture treated plates to generate adherent monolayer cultures. A third stem cell culture format was generated by culturing single cells in standard serum-free media (Neurobasal-A media containing B27, Glutamax, L-glutamine, HEPES, EGF, and FGF [Gibco]) referred to as "neurospheres." Both EPN cell lines were passaged up to 20 times, however, later passages (>20) in monolayer format tended to exhibit a decreased rate in growth and more elongated morphology with lower cell density. As such, these EPN cell lines are not as stable as other brain tumor cell lines established from more aggressive tumors, for example U251-MG and Daoy. Adult glioblastoma (GBM) cell line U87 and atypical teratoid/rhabdoid tumor (AT/RT) cell line 737 were also cultured in monolayer and 3D culture serum media formats, as well as neurosphere serum-free formats. All patient samples were obtained from Children's Hospital Colorado in accordance with local and federal human research protection guidelines and Institutional Review Board regulations (COMIRB 95-500 and #09-0906). All experiments described were conducted within the first 10 passages of 811 and 928 in all culture formats.

Immunohistochemistry

Antibody immunostaining of 5-μm formalin-fixed, paraffin-embedded tumor tissue sections was performed for calcyphosine (Novus, Littleton, CO; NBP1-91746; 1:200 dilution), C9orf24 (Sigma, St. Louis, MO; HPA053008, 1:20 dilution), epithelial membrane antigen (EMA), clone E29 (DAKO Corp., Carpinteria, CA; M0613; 1:100 dilution), glial fibrillary acidic protein (GFAP) (DAKO Corp.; M0761; 1:100 dilution), and MIB-1 (DAKO Corp., monoclonal, 1:400 dilution). For calcyphosine and C9orf24, antigen retrieval required 10 mM sodium citrate pH 6.0 for 10 minutes at 110°C. High pH antigen retrieval was performed for GFAP and MIB-1 and Ventana CC1 antigen retrieval for EMA. All immunostained sections were counterstained with hematoxylin.

Cytogenetics

Karyotype analysis was performed at the Colorado Genetics Laboratory (Denver, CO). Monolayer cell cultures in log-phase growth were harvested by standard cytogenetics methods after mitotic arrest with colcemid (0.05 mg/mL) for 4 hours and enzymatic dispersal with trypsin/EDTA. Cell suspensions were spotted onto microscope glass slides, and G-banding metaphase spreads images were acquired and analyzed. At least 20 metaphases were analyzed for each cell line, and karyotyping designation followed the International System for Human Cytogenetic Nomenclature (13).

Gene Expression Microarray Analysis

RNA was isolated from samples and analyzed to generate transcriptomic microarray profiles using Affymetrix HG-U133 Plus 2 GeneChip microarrays (Affymetrix, Santa Clara, CA) as previously described (14). A panel of established cell lines and short-term cultures were included for comparative purposes, including 3 AT/RT (737, a cell line that was previously established in our laboratory, BT12 and BT16) (15), 3 GBM (pediatric line SF188 and adult lines U251-MG and U87 [ATCC]), 2 medulloblastoma (MED) (Daoy, ONS76), 1 normal human astrocyte short-term culture (Lonza, Allendale, NJ), and 1 fibroblast short-term culture established from CNS surgical material.

Additional patient samples were used for comparative transcriptomic analyses. A total of 25 primary EPN tumor samples were studied, including 10 PF group A, 10 group B, and 5 ST that had been classified by molecular group in a prior study (5). We also included the 4 recurrent tumor samples from which the cell lines were derived. Fifty-five additional samples, including normal brain or other primary brain tumors (10 AT/RT, 10 GBM, 15 MED, and 10 pilocytic astrocytoma) were used for further comparison. Tumor specimens were classified according to WHO international histological tumor classification (9). Nonneoplastic brain samples (n = 10) were collected from routine epilepsy surgery (1 frontal lobe) or autopsy (4 cerebellum, 2 frontal lobe, 1 occipital lobe, and 1 temporal lobe) at Children's Hospital Colorado. One cerebellum sample was from a commercial source (Ambion, Naugatuck, CT). Patient samples were collected at the time of surgery and snap frozen in liquid nitrogen, fixed in formalin-fixed paraffin-embedded tissue, and used to establish cell cultures as described above.

Data Transformation and Analysis

Transcriptomic data was processing, unsupervised hierarchical clustering and gene ontology analysis as described previously (16). These data have been deposited in the National Center for Biotechnology Information Gene Expression Omnibus (GEO) database (17) and are publicly accessible through GEO Series accession number GSE86574 (http://www.ncbi.nlm.nih.gov/geo/query/acc.cgi?acc=GSE86574).

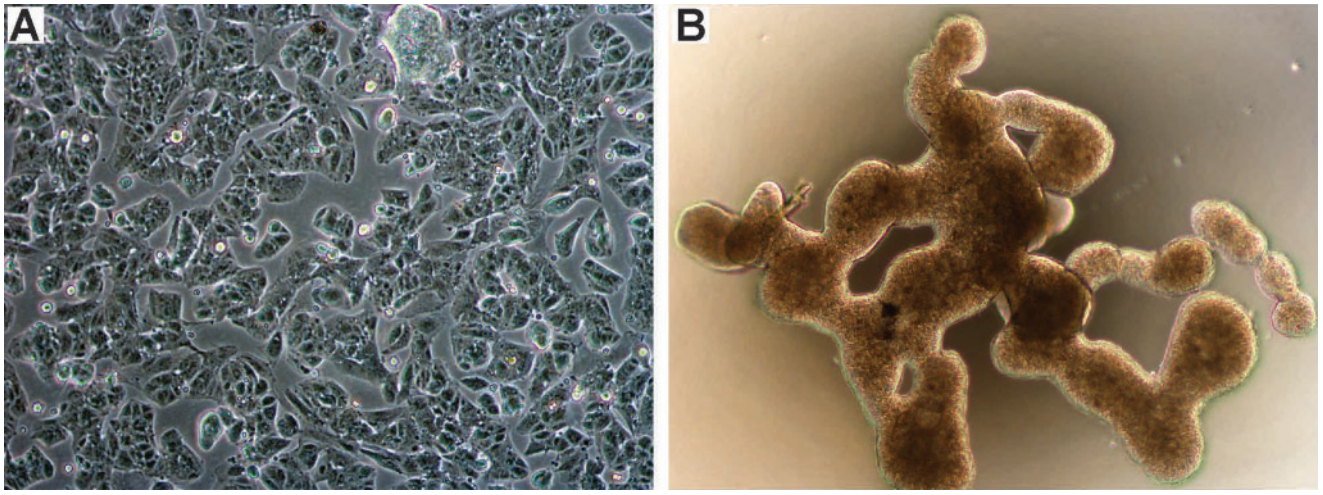

FIGURE 1. Morphology of EPN cell lines grown in monolayer and 3D culture formats. Phase contrast microscopy images showing appearance of cell line 811 grown in (**A**) monolayer (unstained, 100×), and (**B**) 3D culture (unstained, 40×).

Statistical Analysis

Statistical analyses were performed using GraphPad Prism (La Jolla, CA) and Excel Microsoft Excel software. For all tests, significance was defined as a $p < 0.05$.

RESULTS

Morphology of EPN Cell Lines Grown In Different Culture Formats

Phase contrast microscopy of EPN cell lines grown in monolayer and 3D formats was performed. The monolayer tissue culture showed complete loss of ependymal architecture with angular discohesive cells and clusters containing well-defined cell borders (Fig. 1A). Culture of both EPN cell lines in FBS supplemented media in ultra-low attachment plates resulted in large nonadherent, multi-cellular aggregates with distinctive interconnected branch-like structures that were maintained throughout multiple (>10) passages (Fig. 1B). This unique branching morphology appears unique to EPN, as ATRT cell line 737 and GBM cell line U87 formed classic neurospheres under similar culture conditions.

Histological Comparison of In Vitro Cell Lines With In Situ Tumor of Origin

Corresponding in situ EPN patient samples and EPN cell lines in monolayer and 3D formats were fixed and paraffin-embedded for hematoxylin and eosin (H&E) staining to examine finer histological features. Both 811 and 928 in situ patient samples were classified as WHO grade III EPN. Sections of the patient's tumors (Fig. 2A; Supplementary Data Fig. S2A, D) revealed classic features of EPN, including syncytial networks of monomorphic cells with round to oval nuclei, speckled chromatin, dot-like nucleoli and perivascular pseudo-rosettes with fibrillary material surrounding the vascular spaces. Both in situ tumors manifested hyper-cellularity, multifocal necrosis, and microvascular proliferation. In hyper-cellular areas, mitoses reached >5 per high-powered field, corresponding to MIB-1 staining rates of 15%–25% (Supplementary Data Fig. S3). This histology was recapitulated in 3D culture format of the same tumor (Fig. 2B; Supplementary Data Fig. S2B, E), with dot-like nucleoli, a pseudo-papillary arrangement, centrally placed fibrillary material, and multifocal necrosis, but with no vasculature. Mitotic levels in 3D culture formats were consistent with those seen in corresponding in situ tumors (Supplementary Data Fig. S3). In contrast, the monolayer culture format (Fig. 2C; Supplementary Data Fig. S2) shows complete loss of architecture although with retained dot-like nucleoli and reduced mitotic rate in comparison to corresponding in situ tumor (Supplementary Data Fig. S3). The reduced mitotic activity observed in monolayer cultures of both cell lines despite propagation in the same media as 3D cultures suggests that maintenance of architecture contributes to proliferation rate in EPN.

We used 2 immunostains routinely employed for pathological diagnosis of EPN (EMA and GFAP) to confirm preservation of EPN characteristics between in situ tumor and corresponding 3D and monolayer culture formats. EPN in situ tumor demonstrated focal, luminal pattern EMA cytoplasmic staining (Fig. 2D) that was conserved in 3D culture format (Fig. 2E). EPN cell lines in monolayer format in vitro, however, showed irregularly increased EMA cytoplasmic positivity when compared to the in situ section (Fig. 2F). EPN in situ tumor demonstrated GFAP immunoreactivity in fibrillary material and perivascular nuclear-free zones (Fig. 2G). EPN cell lines cultured in 3D format demonstrated accentuated GFAP expression within the fibrillary material (Fig. 2H), but this was almost completely absent in EPN monolayer (Fig. 2I).

Conventional cytogenetic analysis of EPN cells lines revealed similar karyotypes to the primary tumors. The predominant clone of 811 harbored a derivative chromosome 6 resulting from a translocation between the long (q) arm of chromosomes 1 and 6 (resulting in 1q+ and loss of 6q), gain of 1 copy of chromosomes 7 and 9, and a deletion of 10q

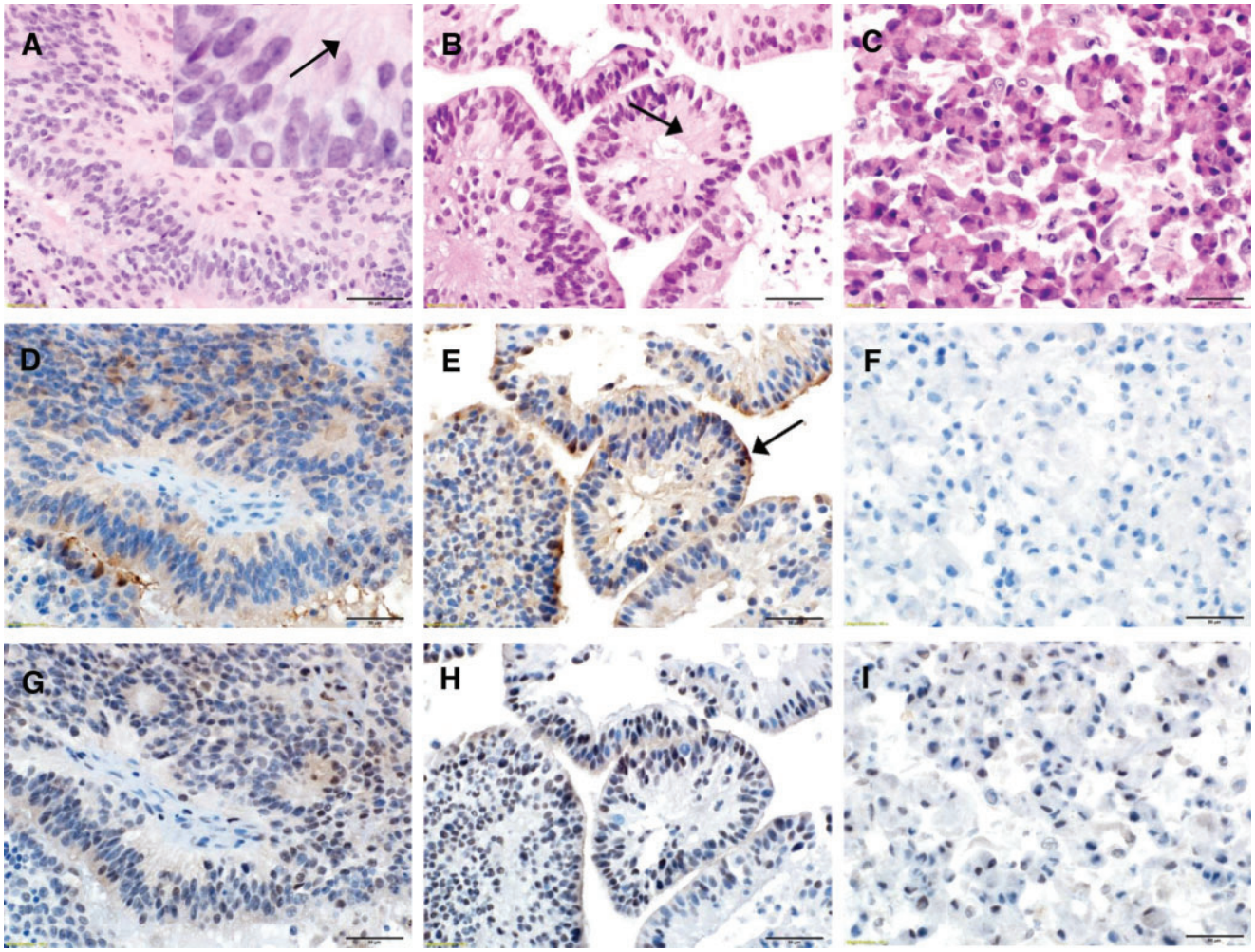

FIGURE 2. Histological comparison of EPN in vitro cell lines with in situ tumor of origin. (**A**) Representative histological images of 811 in situ patient tumor revealing classic features of EPN including syncytial networks of monomorphic cells with round to oval nuclei, speckled chromatin, and perivascular pseudorosettes. The inset magnification highlights fibrillary material (arrow) surrounding the vascular spaces (H&E). (**B**) 811 3D culture in vitro format derived from the same tumor demonstrates similar appearing cells with regularly arranged monomorphic nuclei with the retention of the syncytial networks but with a pseudopapillary arrangement and centrally placed fibrillary material (arrow) and no vasculature (H&E). (**C**) 811 cells grown in monolayer format show complete loss of architecture, syncytial networks, and the fibrillary material with discohesive cells and well-defined cell borders (H&E). (**D**) EMA immunoreactivity in 811 in situ tumor demonstrating a blush of dot like cytoplasmic staining that was conserved in (**E**) 811 3D culture format. (**F**) By contrast, 811 grown in monolayer format showed irregularly increased cytoplasmic positivity when compared to the in situ section (EMA). (**G**) Immunoreactivity for GFAP was observed in fibrillar material and perivascular nuclear-free zones of 811 in situ tumor. (**H**) 3D format demonstrated accentuated GFAP expression within the fibrillar material (I) that was almost completely lost in the monolayer culture (GFAP). (Panels **A–I**: 400× magnification, scale bar = 50 μm).

(Table 1A). Cell line 928 also harbored translocation between long arms of chromosome 1 and 6, also resulting in 1q+ and loss of 6q, but with no other abnormal chromosomes.

EPN Cell Lines Harbor Molecular Group a Transcriptional Profiles That Correlate With Chromosomal Gains/Losses

NMF clustering analysis of transcriptional profiles of 811 and 928 EPN monolayers revealed that they both clustered with EPN molecular group A (Supplementary Data Fig. S1). Further transcriptomic analysis was performed to identify EPN cell line-specific gene expression patterns. Transcriptomic profiles from cell lines grown as monolayer for 811 (n = 4) and 928 (n = 2) were compared to a panel of nonEPN brain tumor cell lines and normal cell short-term cultures, namely ATRTs (BT12, BT16, and 737, n = 5), GBM (SF188, U251, and U87; n = 3), MED (Daoy, ONS76; n = 2), normal human astrocytes (n = 1), and fibroblasts (n = 1). Genes that were significantly differentially expressed >4-fold in either direction were subject to DAVID analysis to identify enrichment or depletion of genes with respect to location on individ-

TABLE 1A. EPN Cell Line Early Passage Karyotype

Cell line 811_5
48, XY, der(6)t(1;6)(q11;q12),+7,+9,del(10)(q22q25)
Cell line 928_3
46, XY, +1der(1;6)(q10;p10)

TABLE 1B. Transcriptomic Enrichment/Depletion Corresponds to Chromosomal Gain/Loss In EPN Cell Lines

Gene Set Category	Location	Fold Enrichment	p Value	FDR
Cell line 811				
Overexpressed Compared To Other Cell Lines (FC > 4; p < 0.05)				
Chromosome	9	2.12	2.76E-20	2.26E-17
Chromosome	7	1.58	6.35E-09	5.21E-06
Chromosome	1	1.37	2.69E-07	2.21E-04
Cytoband	7q22.1	3.68	7.09E-06	0.0112
Cytoband	9p24.1	6.91	8.44E-06	0.0133
cytoband	9q32	5.40	2.61E-05	0.0411
Under Expressed Compared To Other Cell Lines (FC > 4; p < 0.05)				
Chromosome	6	1.51	5.36E-06	0.00440
Cytoband	6q21	4.85	6.15E-06	0.00932
Cell line 928				
Overexpressed Compared To Other Cell Lines (FC > 4; p < 0.05)				
Chromosome	1	1.38	9.76E-06	0.00801
Under Expressed Compared To Other Cell Lines (FC > 4; p < 0.05)				
Chromosome	6	1.51	5.36E-06	0.00440
Cytoband	6q21	4.85	6.15E-06	0.00932

FC, fold change; FDR, false discovery rate.

ual chromosomes or cytobands. Analysis of transcriptomic enrichment in 811 versus other cell lines demonstrated significant overexpression of chromosome 9, 7, and 1 located genes (Table 1B). Conversely, genes under-expressed in 811 corresponded to those on chromosome 6 and cytoband 6q21. This enrichment and depletion of chromosomal specific gene expression correspond directly to chromosomal gains and losses seen in the 811 karyotype (Table 1A). Analysis of 928 also showed specific enrichment of genes coded in chromosome 1 and a loss of genes coded within chromosome 6, corresponding to gains and losses seen in the 928 karyotype (Table 1A). In summary, chromosomal aberrations correspond to observed transcriptomic effects in both EPN cell lines.

Superior Fidelity of EPN Cell Lines Maintained In 3D Culture Format

Histologic analysis of in vitro EPN cell lines identified features that recapitulate human EPN tumor histology in situ, most notably formation of canal-like features in 3D cultures (Fig. 2). To further assess the fidelity of EPN cell lines versus EPN tumor in situ, we compared their transcriptomic profiles. Transcriptomic profiles of 26 in vitro cultures and 84 in situ samples (including a panel of pediatric brain tumors and normal brain types) were subjected to unsupervised hierarchical clustering. In this analysis, samples segregated into 2 main groups: an in vitro cluster and a second larger cluster that included all in situ brain tumor and normal brain (Fig. 3A). The second group separated into subclusters that showed concordance to diagnosis. Monolayer formats of 811 and 928 clustered within the main in vitro cluster containing all other brain tumor cell lines. However, 3D cultures of 811 and 928 clustered within the PF EPN in situ subcluster, and more specifically alongside the in situ tumor samples from which they were established. Interestingly, other 3D cultures generated from adult GBM (U87) and pediatric AT/RT (737) clustered within the main in vitro cell culture group and not with the corresponding in situ tumor samples. Unexpectedly, when cultured under nonadherent conditions using serum-free stem cell culture conditions, which are generally considered to generate higher fidelity in vitro models, 811 did not cluster with primary in situ tumor but instead with in vitro EPN monolayer.

A second transcriptomic analysis was performed to assess conservation of EPN-specific gene expression between EPN cell cultures and in situ tumor. EPN monolayer cell line-specific gene expression signatures were measured by comparing EPN monolayer gene expression profiles from both cell lines to nonEPN in vitro monolayer culture gene expression. p Values were used to quantify the difference in expression of individual genes between the 2 groups for each probe set ($n = 54\,675$). p Values were converted to Log10 values and then, to assign directionality, were given a negative value if overexpressed in EPN versus others and a positive value if under expressed in EPN versus others. For comparison, an in situ EPN tumor gene expression profile was generated by comparing EPN ($n = 29$) to other tumor types ($n = 55$), and the gene expression signature was assigned directionality as described above. Correlation (Pearson's R) between EPN monolayer and EPN in situ tumor was then measured using Prism statistical software. The same approach was used to generate an EPN 3D culture-specific gene expression signature that could be compared with EPN in situ tumor. EPN monolayer and in situ tumor gene expression profiles showed a positive correlation (Pearson's $R = 0.25$; $p < 0.0001$) (Fig. 3B). The significant overlap in gene expression patterns between in vitro monolayer and in situ EPN indicates conservation of underlying EPN-specific pathobiology, despite the transcriptomic disparities identified by hierarchical clustering. EPN 3D culture showed an even stronger correlation with EPN in situ tumor (Pearson's $R = 0.5$; $p < 0.0001$) (Fig. 3C) further confirming the greater fidelity of 3D culture to in situ tumor.

In Situ EPN Cilia Related Gene Signature Is Conserved In 3D Culture

Transcriptional comparisons demonstrate preservation of gene expression patterns between EPN in vitro cell cultures and in situ tumor. We further explored these similarities to identify common biological processes that underlie conserved features. Ontological gene set enrichment defined by Gene Ontology GOTerms was measured in genes that were significantly overexpressed greater that 4-fold in EPN in situ tumor, 3D cultures, and monolayers. The top 10 enriched GOTerm gene sets ranked by false discovery rate were compared (Table 2). This analysis

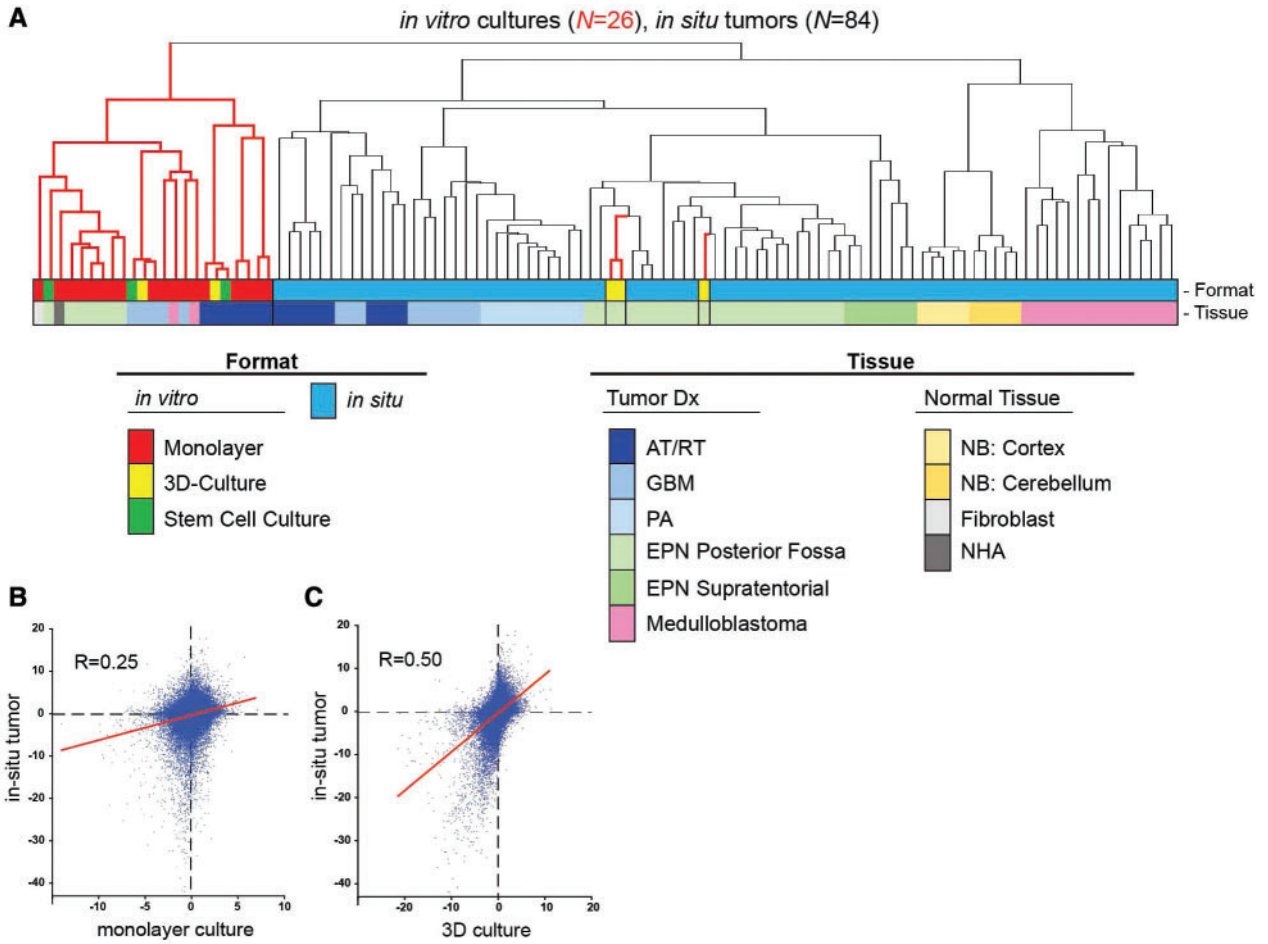

FIGURE 3. Fidelity of EPN cells cultured in 3D format with EPN in situ tumor. (**A**) Unsupervised clustering of transcriptomic profiles of 84 in situ tumor and 26 in vitro cultures. Dendrogram branch colors correspond to in vitro (red) and in situ (black) samples. Dot plots portraying transcriptome signature correlation of (**B**) monolayer, and (**C**) EPN 3D culture, with EPN in situ tumor. Axes are log10 of p values of expression differences for all transcriptomic probe sets ($n = 54\,675$) between EPN and nonEPN samples that have been assigned directionality (negative = overexpressed in EPN; positive = under expressed in EPN). Linear regression lines are shown in red.

indicated that the 2 predominant gene sets enriched in EPN in situ tumor versus other in situ pediatric brain tumor types are those associated with cilia and extracellular matrix. These EPN specific gene set enrichments were also observed in 3D cultures of EPN cell lines, specifically 8 of 10 gene sets common between EPN in situ tumor and 3D culture related to ciliary function and extracellular matrix. EPN monolayer cultures were not as highly conserved but still shared 5 of 10 EPN in situ tumor enriched gene sets. Specifically, monolayers showed accentuated enrichment of extracellular matrix associated gene expression, a hallmark of EPN in situ tumor.

Calcyphosine and C9orf24, Epithelial Cell-Associated Proteins, Are Signatures of EPN In Situ Tumor and Are Conserved In 3D Culture Format

In a new analysis, we identified hallmark genes of EPN in situ tumor by comparison with in situ nonEPN tumors and nonneoplastic brain samples (Supplementary Data Table S1). We then examined expression of these genes in in vitro 3D and monolayer cultures. Conservation of EPN in situ hallmark genes was seen in 3D cultures but to a lesser extent in monolayers. EPN in situ hallmark genes *calcyphosine* and *C9orf24* were selected for further study by immunohistochemstry, based on their conservation in 3D cultures and availability of effective antibodies. Calcyphosine and C9orf24 each have documented roles in cilia formation and function (18–20). Localization and expression of these proteins was examined in 3D and monolayer cell cultures and corresponding in situ tumor samples of both 811 and 928 (Fig. 4). 3D, but not monolayer, cultures retain calcyphosine immunoreactivity, as seen in corresponding in situ tumor (Fig. 4A–C). C9orf24 expression was restricted to the nucleus in EPN tumor in situ. This expression pattern was retained in 3D culture but reduced in monolayer cultures (Fig. 4D–F). Collectively, gene and protein expression analyses demonstrate that cilia-related gene and protein expression is a predominant biological hallmark

TABLE 2. Gene Ontology Analyses of Genes Overexpressed in EPN In Situ Tumor, 3D Culture and Monolayer In Vitro Formats*

GOTerm Annotation	GOTerm ID	Fold Enrichment	p Value	FDR
Cilium	5929	3.63	8.12E-17	1.55E-13
Axoneme	5930	5.60	1.50E-13	2.18E-10
Extracellular matrix	31012	2.29	1.72E-13	2.49E-10
Extracellular region part	44421	1.69	5.10E-13	7.38E-10
Biological adhesion	22610	1.84	5.27E-13	9.82E-10
Cell adhesion	7155	1.83	1.01E-12	1.88E-09
Proteinaceous extracellular matrix	5578	2.30	1.13E-12	1.64E-09
Cell projection	42995	1.82	1.49E-12	2.16E-09
Microtubule basal body	5932	5.36	6.18E-11	8.94E-08
Cell projection part	44463	2.40	1.21E-10	1.76E-07
Overexpressed in EPN 3D Culture Versus Other Cell Lines (FC > 4; p < 0.05)				
Cell adhesion	7155	1.94	2.19E-14	4.04E-11
Biological adhesion	22610	1.94	2.50E-14	4.64E-11
Extracellular matrix	31012	2.31	1.56E-12	2.25E-09
Cell projection	42995	1.87	1.63E-12	2.35E-09
Cell projection organization	30030	2.24	2.94E-12	5.43E-09
Extracellular region part	44421	1.67	3.28E-11	4.72E-08
Proteinaceous extracellular matrix	5578	2.21	2.92E-10	4.20E-07
Cilium	5929	3.05	3.75E-10	5.39E-07
Cell morphogenesis	902	2.12	4.32E-10	7.99E-07
Cell projection part	44463	2.41	7.19E-10	1.03E-06
Overexpressed in EPN Monolayer Versus Other (FC > 4; p < 0.05)				
Extracellular matrix	31012	2.86	2.18E-34	3.22E-31
Proteinaceous extracellular matrix	5578	2.84	1.89E-31	2.79E-28
Extracellular region part	44421	1.89	1.80E-27	2.66E-24
Cell adhesion	7155	2.06	1.16E-26	2.18E-23
Biological adhesion	22610	2.05	1.43E-26	2.68E-23
Extracellular structure organization	43062	3.13	6.93E-21	1.30E-17
Extracellular matrix part	44420	3.50	1.12E-19	1.65E-16
Extracellular matrix organization	30198	3.44	4.62E-17	8.65E-14
Extracellular region	5576	1.41	1.73E-15	2.62E-12
Skeletal system development	1501	2.20	2.85E-15	5.41E-12

FC, fold change; FDR, false discovery rate.
*The top 10 enriched ontologies ranked according to FDR (q value) are shown.

of EPN that was conserved between 3D cultures and in situ tumors.

DISCUSSION

A Review of the Literature Highlights the Rarity of EPN Cell Lines

EPN is a childhood brain tumor that exhibits a high rate of recurrence despite aggressive therapy.

Preclinical development of novel therapies has been stymied by a near complete lack of appropriate disease models. In vitro EPN models have been reported sporadically in the literature, though the majority describe short-term cultures (passaged fewer than 10 times) that were predominantly established from ST EPN (21–24). Yu et al described a well-characterized permanent EPN cell line generated from a ST EPN recurrence that has been passaged over 70 times (25). Subcutaneous xenograft mouse models have also been described (26–28). One such study reported a xenograft model derived from a PF EPN recurrence with 1q+ and loss of chromosome 6 on which a number of preclinical studies were performed (26, 29, 30). Here, we describe 2 novel EPN cell lines, 811 and 928, that represent the most aggressive form of this disease. Both lines were generated from intracranial metastatic recurrences of PF EPN that harbor 1q+ and molecular group A characteristics, both prognostic markers of high-risk in EPN. Our success in establishing these lines potentially stems from altered biology that confers more favorable establishment: 811 and 928 were derived from tumor that is multiply recurrent and collected from sites of intracranial metastasis rather than primary tumor. In contrast, our laboratory has attempted to establish cell lines from first occurrence EPN cases for almost 20 years (~50 cases), none of which yielded a stable cell line. We are currently trying to optimize xenograft models using our cells lines. We have had some successful xenografts into the ventricular spaces as confirmed by MRI imaging, however, we have not been able to have a consistent rate of success within each study.

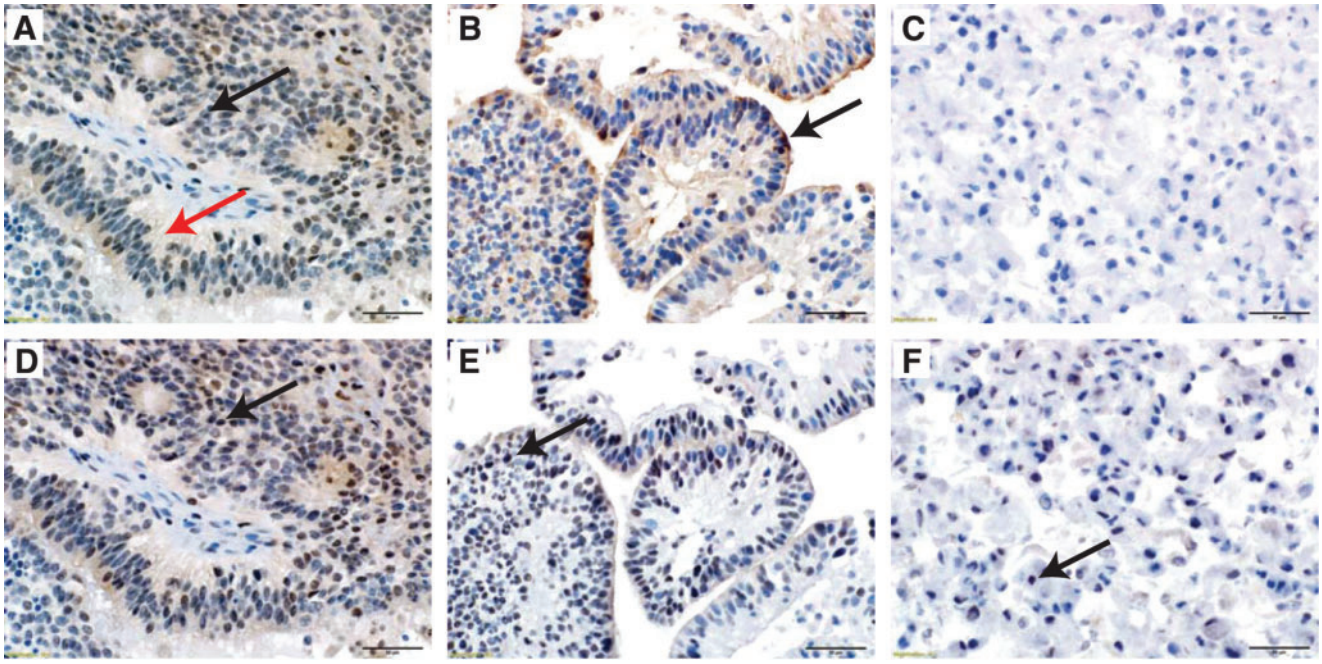

FIGURE 4. Conservation of EPN-specific cilia-associated proteins, calcyphosine and C9orf24, in EPN in situ tumor and 3D culture format. Representative images of (**A**) section of 811 in situ tumor with cytoplasmic (black arrow) and fibrillary material (red arrow) immunoreactivity for calcyphosine. (**B**) 811 3D culture suspension retains the calcyphosine immunoreactivity within the cytoplasm and fibrillary material with an additional accentuation at the outer surface of the pseudopapillary structures (arrow). (**C**) 811 monolayer culture demonstrates complete loss of calcyphosine expression. (**D**) Serial step section of the same in situ 811 tumor with nuclear immunoreactivity for C9orf24 (arrow). (**E**) 811 3D culture suspension retains the C9orf24 nuclear immunoreactivity (arrow). (**F**) 811 monolayer culture demonstrates partial loss of C9orf24 immunoreactivity (arrow). All images: hematoxylin counterstain, 400× magnification, scale bars = 50 μm.

EPN Cell Lines 811 and 928 Show Fidelity With High-Risk Posterior Fossa EPN Primary Tumor

Both cell lines exhibited a derivative chromosome 6 resulting from translocation between chromosomes 1q and 6q. Cell line 811 harbored additional gains of chromosomes 7 and 9. Transcriptomic analysis of cell lines revealed a corresponding enrichment and/or depletion of expression in genes associated with these chromosomal aberrations that were specific for each cell line. This "chromosomal dosage" effect may imply that the phenotypic effect of copy number gain or loss drives aggressiveness in EPN that is associated with 1q gain. Correlation of copy number variation with gene expression levels was recently described in a meta-analysis of several thousand cancer mRNA transcriptomes with known somatic copy number alterations (31). After correcting for nongenetic transcription expression, this cancer-wide study showed that gene expression correlated positively with copy number. Our finding that EPNs demonstrate "gene dosage effect" provides strong rationale for follow-up investigation in the search for candidate driver genes. Such an approach was used to screen areas of copy number gain and loss in an in vivo mouse model of ST EPN, which identified novel EPN-specific oncogenes and tumor suppressors (32). Similarly, the EPN cell lines described in this study provide a model in which siRNA or CRISPR pools could be focused to conserved areas of chromosomal alteration, notably 1q gain and 6q loss, for high-throughput screening of oncogenic drivers in high-risk PF EPN.

EPN cell lines differed in their fidelity with primary disease depending on culture format, which has implications on the utility of cell lines as a relevant EPN model. Both 811 and 928 grouped with other pediatric (and adult) cell lines in their adherent and serum-free neurosphere formats by transcriptomic hierarchical clustering analysis. However, 3D cultures, despite propagation in high serum media, showed greater transcriptomic similarity to primary disease, grouping with EPN primary tumor samples. Analysis of gene function associated with primary EPN and different cell culture formats showed cilia related genes to be the predominant ontology associated with both primary and 3D culture. Consistent with this, 3D cultures showed conservation of EPN in situ tumor hallmark genes *calcyphosine* and *C9orf24*, both epithelial cell and cilia-associated genes. Proteomic analysis of EPN had previously identified calcyphosine as an EPN-specific marker that was not related to histologic grade or location of the EPNs, but was predominantly shown in tumors with epithelial differentiation (19). Consistent with this prior study, we saw calcyphosine protein expression in epithelial cells of both in situ and 3D culture EPN. C9orf24 has previously been described as a regulator of ciliogenesis and/or the intracellular function of cilia (20). This protein was expressed similarly to calcyphosine,

where expression of C9orf24 was found in columnar epithelial cells in our in situ tumor and 3D culture format. Despite recent research designating decreased ciliogenesis as a biomarker for aggressive forms of EPN (18), ciliogenesis is still a predominant signature of and likely plays a crucial role in the specific biology of EPN. This ciliogenesis-associated gene signature is almost certainly due to retention of ciliogenesis-associated properties of ependyma, the putative cell of origin of EPN. Although ciliogenesis is "increased" in our hallmark signature of EPN, we suspect that the level of ciliogenesis in EPN is decreased compared to normal ependymal. Monolayer cells lack the expression of these epithelial cell-related proteins, likely due to the absence of complex multicellular morphology, including epithelial differentiation seen in corresponding primary and 3D cultures. Collectively, these data suggest that the presence of epithelial cell morphology in 3D cultures is the main determinant of fidelity with in situ tumor in EPN. Furthermore, the 3D culture format may be superior to monolayer cultures for preclinical therapeutic testing in EPN. Despite this, the monolayer format still has value, as it maintains other key EPN-specific biological phenotypes. Notably, transcriptomic studies showed that EPN monolayers clustered with high-risk PF molecular group A and conservation of extracellular matrix gene expression, a hallmark of in situ EPN. Furthermore, monolayer cells demonstrate strong correlation of copy number gains and losses with gene expression. This is important given that monolayer cells are better suited for high-throughput screening and downstream studies than 3D cultures.

Characterization of our 1q+ group A EPN cell lines sheds light on the underlying biology of EPN and demonstrates their value as models for preclinical testing and development of novel therapeutic strategies for this devastating disease.

ACKNOWLEDGEMENTS

The authors appreciate the contribution to this research made by E. Erin Smith, HTL(ASCP)CMQIHC, Allison Quador, HTL(ASCP)CM, and Jessica Arnold HTL(ASCP)CM of the University of Colorado Denver Histology Shared Resource.

REFERENCES

1. Gajjar A, Packer RJ, Foreman NK, et al. Children's Oncology Group's 2013 blueprint for research: central nervous system tumors. Pediatr Blood Cancer 2013;60:1022–6
2. Korshunov A, Witt H, Hielscher T, et al. Molecular staging of intracranial ependymoma in children and adults. J Clin Oncol 2010;28:3182–90
3. Kilday JP, Rahman R, Dyer S, et al. Pediatric ependymoma: biological perspectives. Mol Cancer Res 2009;7:765–86
4. Parker M, Mohankumar KM, Punchihewa C, et al. C11orf95-RELA fusions drive oncogenic NF-kappaB signalling in ependymoma. Nature 2014;506:451–5
5. Hoffman LM, Donson AM, Nakachi I, et al. Molecular sub-group-specific immunophenotypic changes are associated with outcome in recurrent posterior fossa ependymoma. Acta Neuropathol 2014;127:731–45
6. Witt H, Mack SC, Ryzhova M, et al. Delineation of two clinically and molecularly distinct subgroups of posterior fossa ependymoma. Cancer Cell 2011;20:143–57
7. Pajtler KW, Witt H, Sill M, et al. Molecular classification of ependymal tumors across all CNS compartments, histopathological grades, and age groups. Cancer Cell 2015;27:728–43
8. Rousseau A, Idbaih A, Ducray F, et al. Specific chromosomal imbalances as detected by array CGH in ependymomas in association with tumor location, histological subtype and grade. J Neurooncol 2010;97:353–64
9. Louis DN, Ohgaki H, Wiestler OD, et al., eds. *WHO Classification of Tumours of the Central Nervous System*. 4th Edition edition. Lyon: International Agency for Research on Cancer, 2016
10. Kilday JP, Mitra B, Domerg C, et al. Copy number gain of 1q25 predicts poor progression-free survival for pediatric intracranial ependymomas and enables patient risk stratification: a prospective European clinical trial cohort analysis on behalf of the Children's Cancer Leukaemia Group (CCLG), Societe Francaise d'Oncologie Pediatrique (SFOP), and International Society for Pediatric Oncology (SIOP). Clin Cancer Res 2012;18:2001–11
11. Mendrzyk F, Korshunov A, Benner A, et al. Identification of gains on 1q and epidermal growth factor receptor overexpression as independent prognostic markers in intracranial ependymoma. Clin Cancer Res 2006;12:2070–9
12. Waziri A, Killory B, Ogden AT 3rd, et al. Preferential in situ CD4+CD56+ T cell activation and expansion within human glioblastoma. J Immunol 2008;180:7673–80
13. Shaffer LG, McGowan-Jordan J, Schmid M. *ISCN: An International System for Human Cytogenetic Nomenclature*. Karger, 2013
14. Donson AM, Birks DK, Barton VN, et al. Immune gene and cell enrichment is associated with a good prognosis in ependymoma. J Immunol 2009;183:7428–40
15. Knipstein JA, Birks DK, Donson AM, et al. Histone deacetylase inhibition decreases proliferation and potentiates the effect of ionizing radiation in atypical teratoid/rhabdoid tumor cells. Neuro Oncol 2012;14:175–83
16. Griesinger AM, Josephson RJ, Donson AM, et al. Interleukin-6/STAT3 pathway signaling drives an inflammatory phenotype in group A ependymoma. Cancer Immunol Res 2015;3:1165–74
17. Ashburner M, Ball CA, Blake JA, et al. Gene ontology: tool for the unification of biology. The Gene Ontology Consortium. Nat Genet 2000;25:25–9
18. Abedalthagafi MS, Wu MP, Merrill PH, et al. Decreased FOXJ1 expression and its ciliogenesis programme in aggressive ependymoma and choroid plexus tumours. J Pathol 2016;238:584–97
19. de Bont JM, den Boer ML, Kros JM, et al. Identification of novel biomarkers in pediatric primitive neuroectodermal tumors and ependymomas by proteome-wide analysis. J Neuropathol Exp Neurol 2007;66:505–16
20. Yoshisue H, Puddicombe SM, Wilson SJ, et al. Characterization of ciliated bronchial epithelium 1, a ciliated cell-associated gene induced during mucociliary differentiation. Am J Respir Cell Mol Biol 2004;31:491–500
21. Hare CB, Elion GB, Houghton PJ, et al. Therapeutic efficacy of the topoisomerase I inhibitor 7-ethyl-10-(4-[1-piperidino]-1-piperidino)-carbonyloxy-camptothecin against pediatric and adult central nervous system tumor xenografts. Cancer Chemother Pharmacol 1997;39:187–91
22. Bobola MS, Jankowski PP, Gross ME, et al. Apurinic/apyrimidinic endonuclease is inversely associated with response to radiotherapy in pediatric ependymoma. Int J Cancer 2011;129:2370–9
23. Guan S, Shen R, Lafortune T, et al. Establishment and characterization of clinically relevant models of ependymoma: a true challenge for targeted therapy. Neuro Oncol 2011;13:748–58
24. Brisson C, Lelong-Rebel I, Mottolese C, et al. Establishment of human tumoral ependymal cell lines and coculture with tubular-like human endothelial cells. Int J Oncol 2002;21:775–85
25. Yu L, Baxter PA, Voicu H, et al. A clinically relevant orthotopic xenograft model of ependymoma that maintains the genomic signature of the primary tumor and preserves cancer stem cells in vivo. Neuro Oncol 2010;12:580–94
26. McLendon RE, Fung KM, Bentley RC, et al. Production and characterization of two ependymoma xenografts. J Neuropathol Exp Neurol 1996;55:540–8

27. Horowitz ME, Parham DM, Douglass EC, et al. Development and characterization of human ependymoma xenograft HxBr5. Cancer Res 1987; 47:499–504
28. Houghton PJ, Adamson PC, Blaney S, et al. Testing of new agents in childhood cancer preclinical models: meeting summary. Clin Cancer Res 2002;8:3646–57
29. Aaron RH, Elion GB, Colvin OM, et al. Busulfan therapy of central nervous system xenografts in athymic mice. Cancer Chemother Pharmacol 1994;35:127–31
30. Friedman HS, Dolan ME, Pegg AE, et al. Activity of temozolomide in the treatment of central nervous system tumor xenografts. Cancer Res 1995;55:2853–7
31. Fehrmann RS, Karjalainen JM, Krajewska M, et al. Gene expression analysis identifies global gene dosage sensitivity in cancer. Nat Genet 2015;47:115–25
32. Mohankumar KM, Currle DS, White E, et al. An in vivo screen identifies ependymoma oncogenes and tumor-suppressor genes. Nat Genet 2015; 47:878–87